Supplement of Atmos. Chem. Phys., 25, 1917–1930, 2025
https://doi.org/10.5194/acp-25-1917-2025-supplement

Atmospheric Chemistry and Physics Open Access

Supplement of

Measurement report: Brown carbon aerosol in rural Germany – sources, chemistry, and diurnal variations

Feng Jiang et al.

Correspondence to: Feng Jiang (feng.jiang@kit.edu) and Harald Saathoff (harald.saathoff@kit.edu)

1. Nitroaromatic compounds and levoglucosan calibration

The calibration of 4-nitrophenol, 4-nitrocatechol, 2-methyl-4-nitropehnol, and 4-methyl-5-nitrocatechol was utilized to characterize the sensitivity of nitro aromatic compounds (NACs). Each NACs was dissolved into methanol to about 10 ng μL^{-1} as a standard NACs solution. Different volume (1, 2, 5, and 10 μL) of the standard NACs solution was deposited on a PTFE filter using an accurate syringe. The deposited filter was heated by FIGAERO-iodide-CIMS with ultra-high purity nitrogen following a thermal desorption. The filters were then desorbed in the same way as for the field samples. Every volume of the standard solution was repeated three times. The sensitivities of our iodide CIMS for 4-nitrophenol, 4-nitrocatechol, 2-methyl-4-nitropehnol, and 4-methyl-5-nitrocatechol were 18 ± 10 cps ppt^{-1}, 11 ± 7 cps ppt^{-1}, 21 ± 11 cps ppt^{-1}, and 21 ± 14 cps ppt^{-1}, respectively (Figure S9). The slopes in Figure S9 are the ratios of measured concentrations by FIGAERO-CIMS from the calibration vs "standard concentrations", where measured concentrations were calculated using a nominal maximum sensitivity of 22 cps ppt^{-1} (Salvador et al., 2021). The average sensitivity of all four NACs was 18 ± 12 cps ppt^{-1}. We used this average sensitivity factor to estimate the concentrations of other potential brown carbon molecules in this study.

We calibrated our FIGAERO-CIMS with the important biomass burning tracer levoglucosan. The calibration method was same as NACs calibration. The sensitivity of levoglucosan was determined 9 ± 3 cps ppt^{-1} (Figure S10). We used the sensitivity of 9 ± 3 cps ppt^{-1} to estimate the concentrations of molecules, which are not identified as potential BrC molecules.

Table S1. Instruments installed in the measurement building number 322 at KIT Campus Nord during the campaign from February 17th – March 16th, 2021.

Measured parameter	**Instrument**
Ambient temperature	WS700 (Lufft GmbH)
Container temperature	WS700 (Lufft GmbH)
Relative humidity	WS700 (Lufft GmbH)
Pressure	WS700 (Lufft GmbH)
Wind speed	WS700 (Lufft GmbH)
Wind direction	WS700 (Lufft GmbH)
Precipitation	WS700 (Lufft GmbH)
Global radiation	WS700 (Lufft GmbH)
O_3	O341M (Environment SA)
NO_2	AS32M (Environment SA)
Particle optical diameter (0.18-18 µm)	OPC FIDAS200 (Palas GmbH)
Black carbon (BC)	AE51 Aethalometer (Aethlabs Inc.)
Black carbon (BC)	MA200 Aethalometer (Aethlabs Inc.)
Black carbon (BC) and brown carbon (BrC)	AE33 Aethalometer (Magee Inc.)
Particle-phase oxygenated organic molecules (intermittent online analysis of filters)	FIGAERO-CIMS (Aerodyne Research Inc.)
Gas phase oxygenated organic molecules (online)	CIMS (Aerodyne Research Inc.)
VOCs/semi-volatile particles	CHARON-PTR-MS (IONCON Analytik GmbH)
Profiles of aerosol and/or cloud backscatter	LIDAR (Raymetrics Inc.)
Particle number	CPC 3789 (TSI Inc.)
Particle size (10-410 nm)	Nanoscan (TSI Inc.)

Table S2. Assignment of 171 potential brown carbon molecules and 7 nitro aromatic compounds (red marks) in the particle phase detected at KIT Campus Nord, including mass, formula, double bond equivalent (DBE), the ratio of O/C, the ratio of H/C, value of C*0.9 and C*0.5, average concentrations, and standard variation.

Number	Mass ($g\ mol^{-1}$)	Formula	DBE	O/C	H/C	C*0.9	C*0.5	Average ($ng\ m^{-3}$)	Std ($ng\ m^{-3}$)
1	75	C2H4O3	1.5	1.5	1.5	1.8	1	0.04	0.02
2	104	C3H4O4	2	1.3	1.3	2.7	1.5	0.82	0.85
3	120	C3H4O5	2	1.7	1.3	2.7	1.5	0.32	0.30
4	152	C3H4O7	2	2.3	1.3	2.7	1.5	0.10	0.05
5	168	C3H4O8	2	2.7	1.3	2.7	1.5	0.12	0.05
6	103	C3H5O3N1	2	1.0	1.7	2.7	1.5	0.08	0.03
7	135	C3H5O5N1	2	1.7	1.7	2.7	1.5	0.17	0.13
8	151	C3H5O6N1	2	2.0	1.7	2.7	1.5	0.16	0.12
9	167	C3H5O7N1	2	2.3	1.7	2.7	1.5	0.11	0.11
10	183	C3H5O8N1	2	2.7	1.7	2.7	1.5	0.25	0.17
11	84	C4H4O2	3	0.5	1.0	3.6	2	0.04	0.02
12	116	C4H4O4	3	1.0	1.0	3.6	2	0.50	0.37
13	132	C4H4O5	3	1.3	1.0	3.6	2	0.43	0.33
14	148	C4H4O6	3	1.5	1.0	3.6	2	0.96	0.94
15	164	C4H4O7	3	1.8	1.0	3.6	2	0.56	0.27
16	179	C4H4O7N1	3	1.8	1.3	3.6	2	0.46	0.11
17	180	C4H4O8	3	2.0	1.0	3.6	2	0.99	0.74
18	99	C4H5O2N1	3	0.5	1.3	3.6	2	0.06	0.02
19	131	C4H5O4N1	3	1.0	1.3	3.6	2	0.11	0.06
20	147	C4H5O5N1	3	1.3	1.3	3.6	2	0.14	0.09
21	163	C4H5O6N1	3	1.5	1.3	3.6	2	0.12	0.07
22	179	C4H5O7N1	3	1.8	1.3	3.6	2	0.31	0.18
23	112	C5H4O3	4	0.6	0.8	4.5	2.5	0.46	0.20
24	192	C5H4O8	4	1.6	0.8	4.5	2.5	0.13	0.06
25	80	C5H4O1	4	0.2	0.8	4.5	2.5	0.15	0.10
26	112	C5H4O3	4	0.6	0.8	4.5	2.5	0.07	0.05
27	128	C5H4O4	4	0.8	0.8	4.5	2.5	0.31	0.20
28	144	C5H4O5	4	1.0	0.8	4.5	2.5	0.62	0.44
29	175	C5H4O6N1	4	1.2	1.0	4.5	2.5	0.17	0.08
30	176	C5H4O7	4	1.4	0.8	4.5	2.5	0.05	0.04
31	192	C5H4O8	4	1.6	0.8	4.5	2.5	0.24	0.12
32	82	C5H6O1	3	0.2	1.2	4.5	2.5	0.07	0.02
33	98	C5H6O2	3	0.4	1.2	4.5	2.5	0.02	0.02
34	127	C5H5O3N1	4	0.6	1.0	4.5	2.5	0.06	0.04
35	114	C5H6O3	3	0.6	1.2	4.5	2.5	0.18	0.06
36	143	C5H5O4N1	4	0.8	1.0	4.5	2.5	0.25	0.16

37	159	C5H5O5N1	4	1.0	1.0	4.5	2.5	0.23	0.15
38	175	C5H5O6N1	4	1.2	1.0	4.5	2.5	0.16	0.08
39	178	C5H6O7	3	1.4	1.2	4.5	2.5	0.19	0.08
40	207	C5H5O8N1	4	1.6	1.0	4.5	2.5	0.21	0.12
41	194	C5H6O8	3	1.6	1.2	4.5	2.5	0.18	0.08
42	114	C5H6O3	3	0.6	1.2	4.5	2.5	0.09	0.05
43	130	C5H6O4	3	0.8	1.2	4.5	2.5	0.76	0.68
44	146	C5H6O5	3	1.0	1.2	4.5	2.5	1.50	1.05
45	162	C5H6O6	3	1.2	1.2	4.5	2.5	0.24	0.38
46	178	C5H6O7	3	1.4	1.2	4.5	2.5	0.35	0.15
47	193	C5H6O7N1	3	1.4	1.4	4.5	2.5	0.15	0.05
48	194	C5H6O8	3	1.6	1.2	4.5	2.5	0.26	0.14
49	209	C5H6O8N1	3	1.6	1.4	4.5	2.5	0.37	0.16
50	129	C5H7O3N1	3	0.6	1.4	4.5	2.5	0.21	0.12
51	145	C5H7O4N1	3	0.8	1.4	4.5	2.5	0.20	0.15
52	161	C5H7O5N1	3	1.0	1.4	4.5	2.5	0.19	0.16
53	177	C5H7O6N1	3	1.2	1.4	4.5	2.5	0.37	0.27
54	193	C5H7O7N1	3	1.4	1.4	4.5	2.5	1.47	1.16
55	209	C5H7O8N1	3	1.6	1.4	4.5	2.5	0.30	0.22
56	225	C5H7O9N1	3	1.8	1.4	4.5	2.5	0.13	0.05
57	236	C6H4O10	5	1.7	0.7	5.4	3	0.18	0.06
58	140	C6H4O4	5	0.7	0.7	5.4	3	0.23	0.18
59	156	C6H4O5	5	0.8	0.7	5.4	3	0.29	0.17
60	171	C6H4O5N1	5	0.8	0.8	5.4	3	0.19	0.10
61	188	C6H4O7	5	1.2	0.7	5.4	3	0.13	0.08
62	220	C6H4O9	5	1.5	0.7	5.4	3	0.10	0.04
63	91	C6H5N1	5	0.0	0.8	5.4	3	0.04	0.02
64	139	C6H5O3N1	5	0.5	0.8	5.4	3	0.77	0.50
65	155	C6H5O4N1	5	0.7	0.8	5.4	3	10.81	11.47
66	171	C6H5O5N1	5	0.8	0.8	5.4	3	0.52	0.59
67	187	C6H5O6N1	5	1.0	0.8	5.4	3	0.12	0.04
68	203	C6H5O7N1	5	1.2	0.8	5.4	3	0.09	0.03
69	190	C6H5O7	4	1.2	1.0	5.4	3	0.15	0.08
70	206	C6H5O8	4	1.3	1.0	5.4	3	0.19	0.08
71	222	C6H5O9	4	1.5	1.0	5.4	3	0.14	0.06
72	126	C6H6O3	4	0.5	1.0	5.4	3	0.08	0.05
73	142	C6H6O4	4	0.7	1.0	5.4	3	0.22	0.15
74	157	C6H6O4N1	4	0.7	1.2	5.4	3	0.28	0.11
75	158	C6H6O5	4	0.8	1.0	5.4	3	1.70	1.19
76	174	C6H6O6	4	1.0	1.0	5.4	3	0.55	0.42
77	206	C6H6O8	4	1.3	1.0	5.4	3	0.51	0.27

78	238	C6H6O10	4	1.7	1.0	5.4	3	0.10	0.03
79	141	C6H7O3N1	4	0.5	1.2	5.4	3	0.13	0.06
80	157	C6H7O4N1	4	0.7	1.2	5.4	3	0.27	0.21
81	173	C6H7O5N1	4	0.8	1.2	5.4	3	0.32	0.20
82	189	C6H7O6N1	4	1.0	1.2	5.4	3	0.31	0.20
83	205	C6H7O7N1	4	1.2	1.2	5.4	3	0.27	0.15
84	221	C6H7O8N1	4	1.3	1.2	5.4	3	0.13	0.06
85	200	C7H4O7	6	1.0	0.6	6.3	3.5	0.06	0.04
86	154	C7H6O4	5	0.6	0.9	6.3	3.5	0.35	0.30
87	170	C7H6O5	5	0.7	0.9	6.3	3.5	0.41	0.27
88	218	C7H6O8	5	1.1	0.9	6.3	3.5	0.21	0.11
89	233	C7H6O8N1	5	1.1	1.0	6.3	3.5	0.21	0.07
90	153	C7H7O3N1	5	0.4	1.0	6.3	3.5	0.31	0.19
91	169	C7H7O4N1	5	0.6	1.0	6.3	3.5	3.29	4.00
92	156	C7H7O4	4	0.6	1.1	6.3	3.5	0.44	0.19
93	185	C7H7O5N1	5	0.7	1.0	6.3	3.5	1.25	1.30
94	172	C7H7O5	4	0.7	1.1	6.3	3.5	0.28	0.12
95	201	C7H7O6N1	5	0.9	1.0	6.3	3.5	0.31	0.16
96	188	C7H7O6	4	0.9	1.1	6.3	3.5	0.26	0.17
97	217	C7H7O7N1	5	1.0	1.0	6.3	3.5	0.30	0.17
98	204	C7H7O7	4	1.0	1.1	6.3	3.5	0.18	0.07
99	233	C7H7O8N1	5	1.1	1.0	6.3	3.5	0.07	0.05
100	220	C7H7O8	4	1.1	1.1	6.3	3.5	0.19	0.08
101	140	C7H8O3	4	0.4	1.1	6.3	3.5	0.13	0.12
102	156	C7H8O4	4	0.6	1.1	6.3	3.5	0.39	0.28
103	172	C7H8O5	4	0.7	1.1	6.3	3.5	2.37	1.69
104	188	C7H8O6	4	0.9	1.1	6.3	3.5	0.93	0.52
105	204	C7H8O7	4	1.0	1.1	6.3	3.5	0.46	0.26
106	220	C7H8O8	4	1.1	1.1	6.3	3.5	0.31	0.20
107	236	C7H8O9	4	1.3	1.1	6.3	3.5	0.31	0.17
108	251	C7H8O9N1	4	1.3	1.3	6.3	3.5	0.09	0.03
109	155	C7H9O3N1	4	0.4	1.3	6.3	3.5	0.53	0.47
110	171	C7H9O4N1	4	0.6	1.3	6.3	3.5	0.30	0.21
111	187	C7H9O5N1	4	0.7	1.3	6.3	3.5	0.32	0.24
112	203	C7H9O6N1	4	0.9	1.3	6.3	3.5	0.66	0.58
113	219	C7H9O7N1	4	1.0	1.3	6.3	3.5	1.12	0.83
114	235	C7H9O8N1	4	1.1	1.3	6.3	3.5	0.36	0.22
115	251	C7H9O9N1	4	1.3	1.3	6.3	3.5	0.27	0.11
116	267	C7H9O10N1	4	1.4	1.3	6.3	3.5	0.18	0.06
117	182	C8H6O5	6	0.6	0.8	7.2	4	0.14	0.09
118	213	C8H7O6N1	6	0.8	0.9	7.2	4	0.32	0.18

119	200	C8H8O6	5	0.8	1.0	7.2	4	0.08	0.08
120	229	C8H7O7N1	6	0.9	0.9	7.2	4	0.23	0.10
121	216	C8H8O7	5	0.9	1.0	7.2	4	0.10	0.05
122	168	C8H8O4	5	0.5	1.0	7.2	4	0.20	0.14
123	184	C8H8O5	5	0.6	1.0	7.2	4	0.79	0.46
124	200	C8H8O6	5	0.8	1.0	7.2	4	0.78	0.42
125	216	C8H8O7	5	0.9	1.0	7.2	4	0.55	0.28
126	231	C8H8O7N1	5	0.9	1.1	7.2	4	0.15	0.05
127	183	C8H9O4N1	5	0.5	1.1	7.2	4	1.65	2.08
128	199	C8H9O5N1	5	0.6	1.1	7.2	4	0.51	0.37
129	215	C8H9O6N1	5	0.8	1.1	7.2	4	0.45	0.26
130	231	C8H9O7N1	5	0.9	1.1	7.2	4	0.39	0.21
131	295	C8H9O11N1	5	1.4	1.1	7.2	4	0.14	0.04
132	228	C9H8O7	6	0.8	0.9	8.1	4.5	0.49	0.19
133	211	C9H9O5N1	6	0.6	1.0	8.1	4.5	0.45	0.45
134	230	C9H10O7	5	0.8	1.1	8.1	4.5	0.32	0.24
135	259	C9H9O8N1	6	0.9	1.0	8.1	4.5	0.27	0.10
136	307	C9H9O11N1	6	1.2	1.0	8.1	4.5	0.13	0.04
137	182	C9H10O4	5	0.4	1.1	8.1	4.5	0.26	0.19
138	198	C9H10O5	5	0.6	1.1	8.1	4.5	0.52	0.38
139	214	C9H10O6	5	0.7	1.1	8.1	4.5	1.53	0.89
140	230	C9H10O7	5	0.8	1.1	8.1	4.5	0.59	0.32
141	262	C9H10O9	5	1.0	1.1	8.1	4.5	0.24	0.13
142	213	C9H11O5N1	5	0.6	1.2	8.1	4.5	0.48	0.34
143	229	C9H11O6N1	5	0.7	1.2	8.1	4.5	0.47	0.37
144	293	C9H11O10N1	5	1.1	1.2	8.1	4.5	0.24	0.09
145	309	C9H11O11N1	5	1.2	1.2	8.1	4.5	0.18	0.06
146	242	C10H10O7	6	0.7	1.0	9	5	0.82	0.43
147	257	C10H11O7N1	6	0.7	1.1	9	5	0.56	0.31
148	273	C10H11O8N1	6	0.8	1.1	9	5	0.36	0.19
149	305	C10H11O10N1	6	1.0	1.1	9	5	0.22	0.09
150	353	C10H11O13N1	6	1.3	1.1	9	5	0.19	0.07
151	282	C11H6O9	9	0.8	0.5	9.9	5.5	0.37	0.15
152	284	C11H8O9	8	0.8	0.7	9.9	5.5	0.50	0.23
153	347	C11H9O12N1	8	1.1	0.8	9.9	5.5	0.16	0.04
154	286	C11H10O9	7	0.8	0.9	9.9	5.5	0.58	0.27
155	285	C11H11O8N1	7	0.7	1.0	9.9	5.5	0.30	0.15
156	301	C11H11O9N1	7	0.8	1.0	9.9	5.5	0.21	0.08
157	349	C11H11O12N1	7	1.1	1.0	9.9	5.5	0.25	0.09
158	256	C11H12O7	6	0.6	1.1	9.9	5.5	0.82	0.56
159	272	C11H12O8	6	0.7	1.1	9.9	5.5	0.85	0.44

160	288	C11H12O9	6	0.8	1.1	9.9	5.5	0.16	0.08
161	287	C11H13O8N1	6	0.7	1.2	9.9	5.5	0.41	0.22
162	303	C11H13O9N1	6	0.8	1.2	9.9	5.5	0.35	0.18
163	319	C11H13O10N1	6	0.9	1.2	9.9	5.5	0.25	0.12
164	300	C12H12O9	7	0.8	1.0	10.8	6	0.94	0.49
165	332	C12H12O11	7	0.9	1.0	10.8	6	0.68	0.27
166	348	C12H12O12	7	1.0	1.0	10.8	6	0.64	0.24
167	282	C13H14O7	7	0.5	1.1	11.7	6.5	0.48	0.32
168	330	C13H14O10	7	0.8	1.1	11.7	6.5	0.83	0.34
169	394	C13H14O14	7	1.1	1.1	11.7	6.5	0.36	0.11
170	345	C13H15O10N1	7	0.8	1.2	11.7	6.5	0.38	0.19
171	393	C13H15O13N1	7	1.0	1.2	11.7	6.5	0.20	0.07
172	326	C14H14O9	8	0.6	1.0	12.6	7	0.12	0.11
173	324	C15H16O8	8	0.5	1.1	13.5	7.5	1.39	1.15
174	356	C15H16O10	8	0.7	1.1	13.5	7.5	1.62	0.57
175	372	C15H16O11	8	0.7	1.1	13.5	7.5	1.01	0.37
176	403	C15H17O12N1	8	0.8	1.1	13.5	7.5	0.24	0.10
177	368	C16H16O10	9	0.6	1.0	14.4	8	0.97	0.37
178	366	C17H18O9	9	0.5	1.1	15.3	8.5	0.24	0.17

Table S3. Assignment of 27 potential brown carbon molecules and 4 nitro aromatic compounds (red marks) in the gas phase detected at KIT Campus Nord, including mass, formula, double bond equivalent (DBE), the ratio of O/C, and the ratio of H/C.

Number	Mass ($g\ mol^{-1}$)	Formula	DBE	O/C	H/C	C*0.9	C*0.5	Average ($ng\ m^{-3}$)	Std ($ng\ m^{-3}$)
1	136	C3H4O6	2	2.0	1.3	2.7	1.5	0.95	0.13
2	151	C3H5O6N1	2	2.0	1.7	2.7	1.5	0.05	0.52
3	84	C4H4O2	3	0.5	1.0	3.6	2	0.39	0.52
4	196	C4H4O9	3	2.3	1.0	3.6	2	0.67	0.28
5	163	C4H5O6N1	3	1.5	1.3	3.6	2	0.21	0.62
6	179	C4H5O7N1	3	1.8	1.3	3.6	2	0.46	0.08
7	208	C5H4O9	4	1.8	0.8	4.5	2.5	0.12	0.10
8	175	C5H5O6N1	4	1.2	1.0	4.5	2.5	0.13	0.09
9	191	C5H5O7N1	4	1.4	1.0	4.5	2.5	0.04	0.06
10	207	C5H5O8N1	4	1.6	1.0	4.5	2.5	0.02	0.08
11	130	C5H6O4	3	0.8	1.2	4.5	2.5	0.02	0.47
12	210	C5H6O9	3	1.8	1.2	4.5	2.5	0.51	1.34
13	177	C5H7O6N1	3	1.2	1.4	4.5	2.5	1.16	0.27
14	193	C5H7O7N1	3	1.4	1.4	4.5	2.5	0.24	0.32
15	139	C6H5O3N1	5	0.5	0.8	5.4	3	0.34	0.32
16	155	C6H5O4N1	5	0.7	0.8	5.4	3	1.16	1.04
17	158	C6H6O5	4	0.8	1.0	5.4	3	0.12	0.12
18	222	C6H6O9	4	1.5	1.0	5.4	3	0.12	0.13
19	238	C6H6O10	4	1.7	1.0	5.4	3	0.06	0.08
20	189	C6H7O6N1	4	1.0	1.2	5.4	3	0.10	0.14
21	205	C6H7O7N1	4	1.2	1.2	5.4	3	0.10	0.07
22	221	C6H7O8N1	4	1.3	1.2	5.4	3	0.07	0.08
23	237	C6H7O9N1	4	1.5	1.2	5.4	3	0.05	0.11
24	153	C7H7O3N1	5	0.4	1.0	6.3	3.5	0.11	0.10
25	169	C7H7O4N1	5	0.6	1.0	6.3	3.5	0.32	0.31
26	203	C7H9O6N1	4	0.9	1.3	6.3	3.5	0.10	0.32
27	219	C7H9O7N1	4	1.0	1.3	6.3	3.5	0.30	0.07
28	235	C7H9O8N1	4	1.1	1.3	6.3	3.5	0.00	0.34
29	184	C8H8O5	5	0.6	1.0	7.2	4	0.34	0.15
30	183	C8H9O4N1	5	0.5	1.1	7.2	4	0.11	0.08
31	262	C9H10O9	5	1.0	1.1	8.1	4.5	0.11	0.00

Table S4. Nitro aromatic compounds in gas phase detected at KIT Campus Nord, including chemical formula, concentration range, and average concentration (mean ± standard deviation).

Molecule	Formula	Concentration range (ng m^{-3})	Average concentrations (ng m^{-3})
4-Nitrophenol	C6H5O3N1	0.01-2.8	0.3 ± 0.3
4-Nitrocatechol	C6H5O4N1	0.01-6.4	1.2 ± 1.0
2-Methyl-4-nitrophenol	C7H7O3N1	0.01-0.7	0.1 ± 0.1
4-Methyl-5-nitrocatechol	C7H7O4N1	0.01-2.0	0.3 ± 0.3
∑NACs	-	0.01-9.3	1.9 ± 1.5

Table S5. Nitro aromatic compounds in particle phase detected at KIT Campus Nord, including chemical formula, mass absorption coefficient (MAC) at 365 nm, concentration range, and average concentration (mean ± standard deviation).

Molecule	Formula	MAC ($m^2 g^{-1}$)*	Concentration range ($ng\ m^{-3}$)	Average concentrations ($ng\ m^{-3}$)
4-Nitrophenol	C6H5O3N1	2.44	0.01-2.3	0.8 ± 0.5
4-Nitrocatechol	C6H5O4N1	7.02	0.3-78.9	10.8 ± 11.5
-	C6H5O5N1	14.00	0.1-5.2	0.5 ± 0.6
2-Methyl-4-nitrophenol	C7H7O3N1	3.15	0.02-1.2	0.3 ± 0.2
4-Methyl-5-nitrocatechol	C7H7O4N1	12.90	0.2-31.7	3.3 ± 4.0
-	C7H7O5N1	14.00	0.1-8.8	1.2 ± 1.3
-	C8H9O5N1	14.00	0.06-2.2	0.5 ± 0.4
∑NACs	-		1-130.2	17.5 ± 18.4

∗ (Xie et al. 2017).

Table S6. Gas to particle phase partitioning coefficients of those semi volatile potential brown carbon molecules which could be measured in both phases with sufficient sensitivity (average and standard deviation).

Number	Formula	Average g/p ratio	Std g/p ratio
1	C3H5O6N1	0.81	0.67
2	C4H4O2	9.7	10.1
3	C4H5O6N1	2.1	1.8
4	C4H5O7N1	1.8	1.8
5	C5H5O8N1	0.8	0.5
6	C5H6O4	0.2	0.4
7	C5H7O6N1	3.2	4.4
8	C5H7O7N1	0.3	0.3
9	C6H6O5	0.1	0.1
10	C6H6O10	1.3	0.9
11	C6H7O6N1	0.4	0.3
12	C6H7O7N1	0.6	0.6
13	C6H7O8N1	0.8	0.4
14	C6H5O3N1	0.5	2.1
15	C6H5O4N1	0.1	0.1
16	C7H7O3N1	0.7	0.4
17	C7H7O4N1	0.3	0.2
18	C7H9O6N1	0.4	0.3
19	C7H9O7N1	0.5	0.6
20	C7H9O8N1	0.4	0.4
21	C8H8O5	0.5	0.3
22	C8H9O4N1	0.3	0.2
23	C9H10O9	0.6	0.4

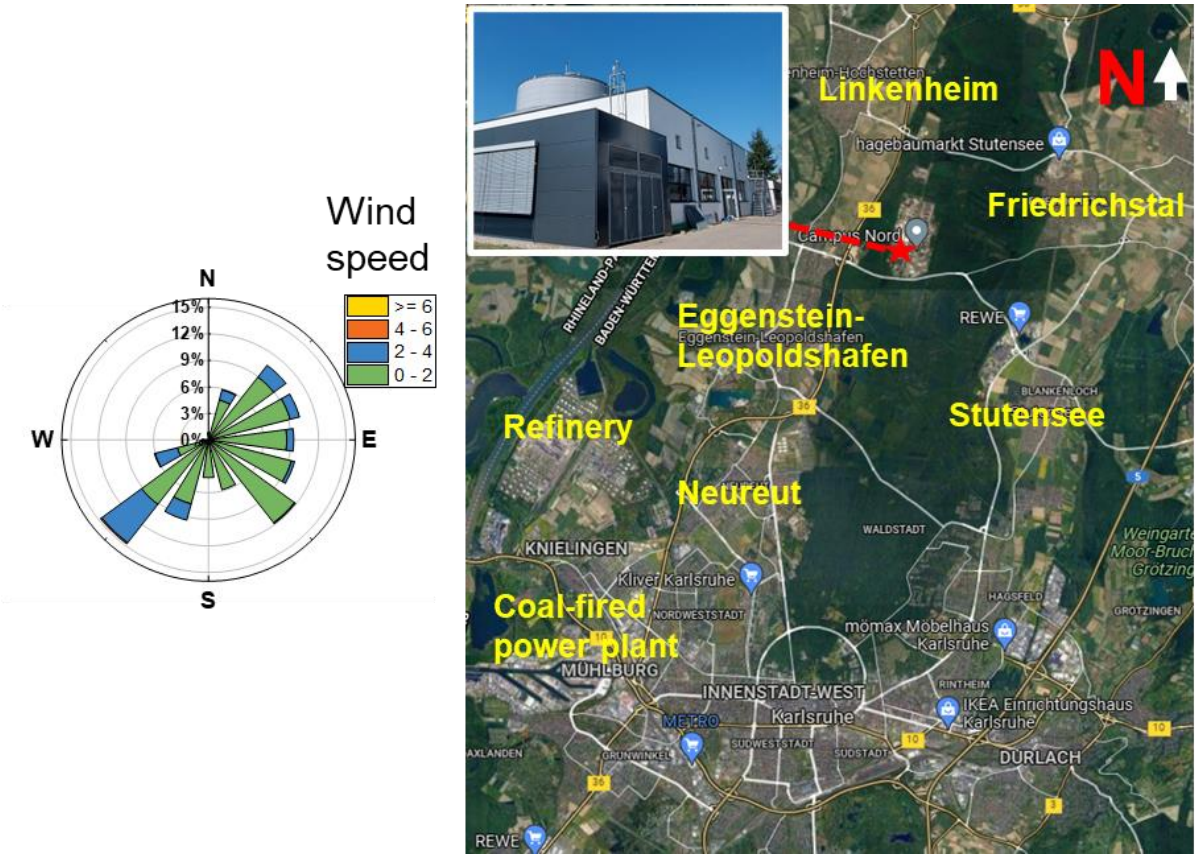

Figure S1. Wind roses (left) pattern, and measurement location map and container picture (right) pattern. Background map courtesy of © Google Maps.

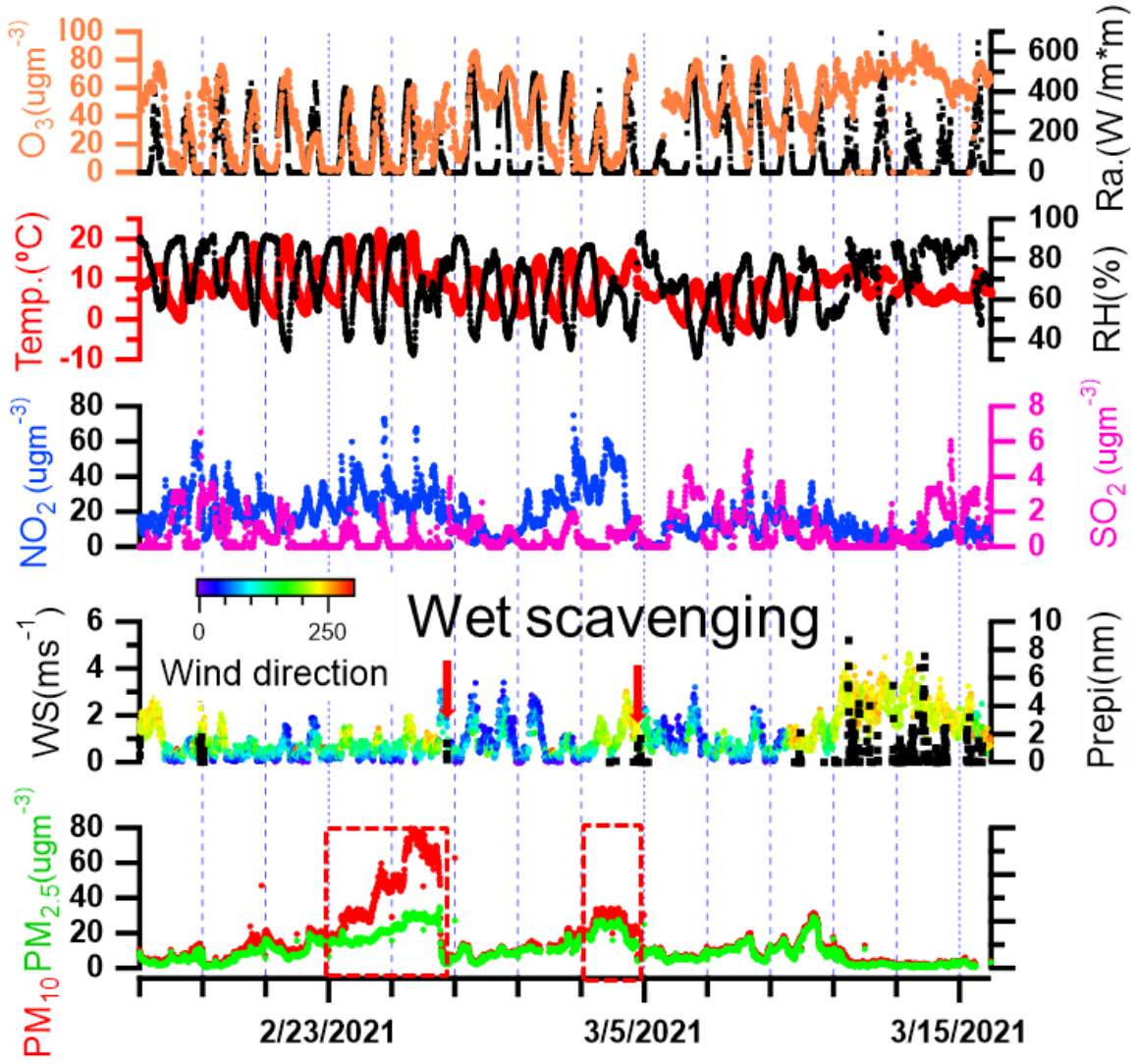

Figure S2 Overview of the meteorological parameters: trace gases (NO_2, O_3, and SO_2), temperature (T), radiation, relative humidity (RH), wind speed (WS), wind direction (WD), precipitation (Precipi), and $PM_{2.5}$ and PM_{10} during the campaign. Red arrows indicate precipitation events leading to substantial removal of aerosol mass e.g. by wet scavenging at the end of periods with high pollution (dashed red boxes). Please note, that the first period was strongly influenced by Saharan dust (Cuevas-Agulló et al., 2023).

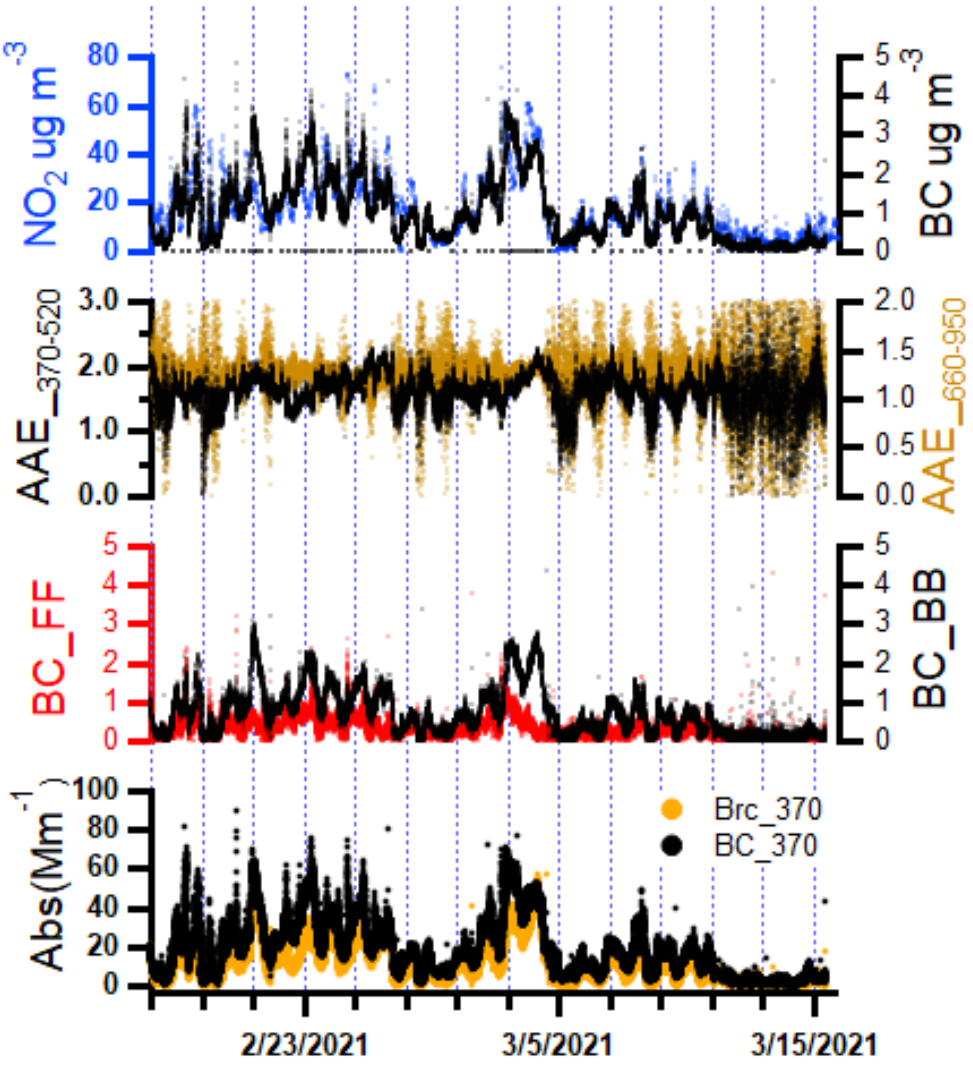

Figure S3. Overview of NO_2 and black carbon (BC), absorption Ångström exponents (AAE) at 370 to 520 nm ($AAE_{370-520}$), AAE at 660 to 950 ($AAE_{660-950}$), BC_FF, BC_BB, Abs_{370} of BrC, and Abs_{370} of BC.

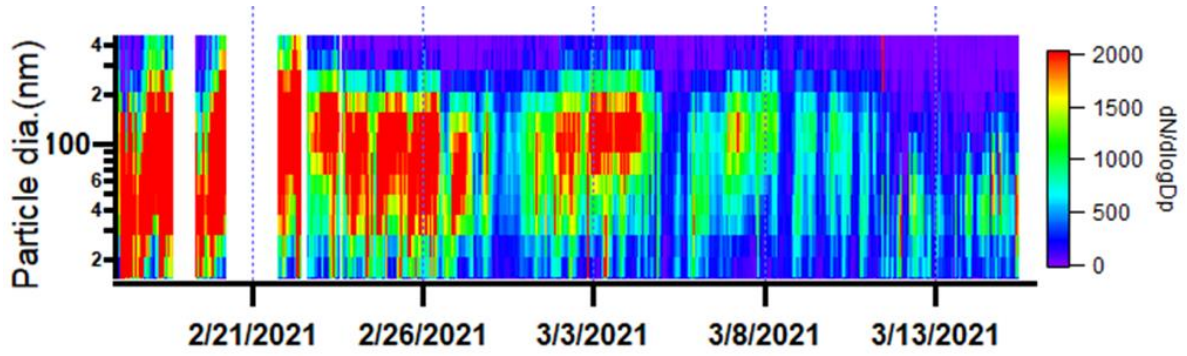

Figure S4. Particle size distributions measured with NanoScan between 10 and 410 nm.

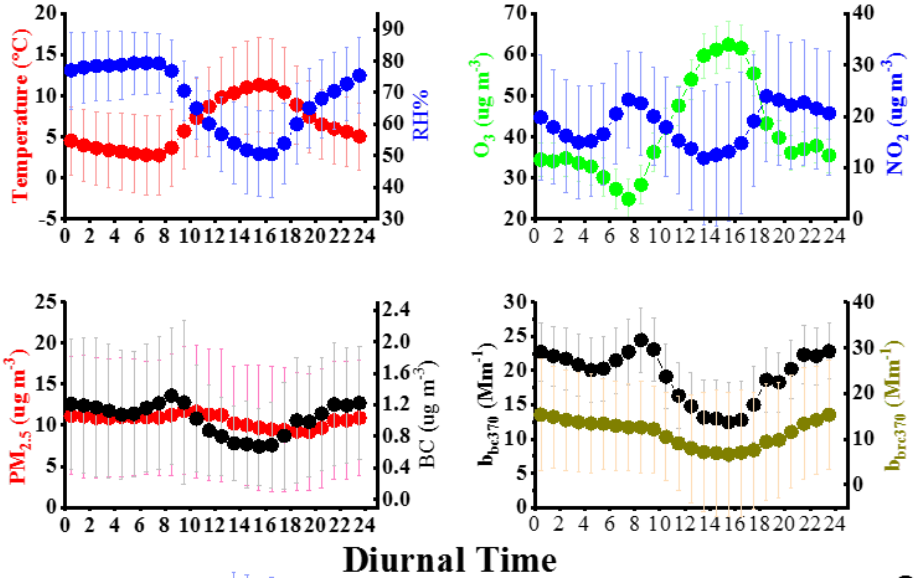

Figure S5. Diurnal variation of temperature, relative humidity, O_3, NO_2, $PM_{2.5}$, BC, b_{bc370} and b_{brc370} for the whole measurement period.

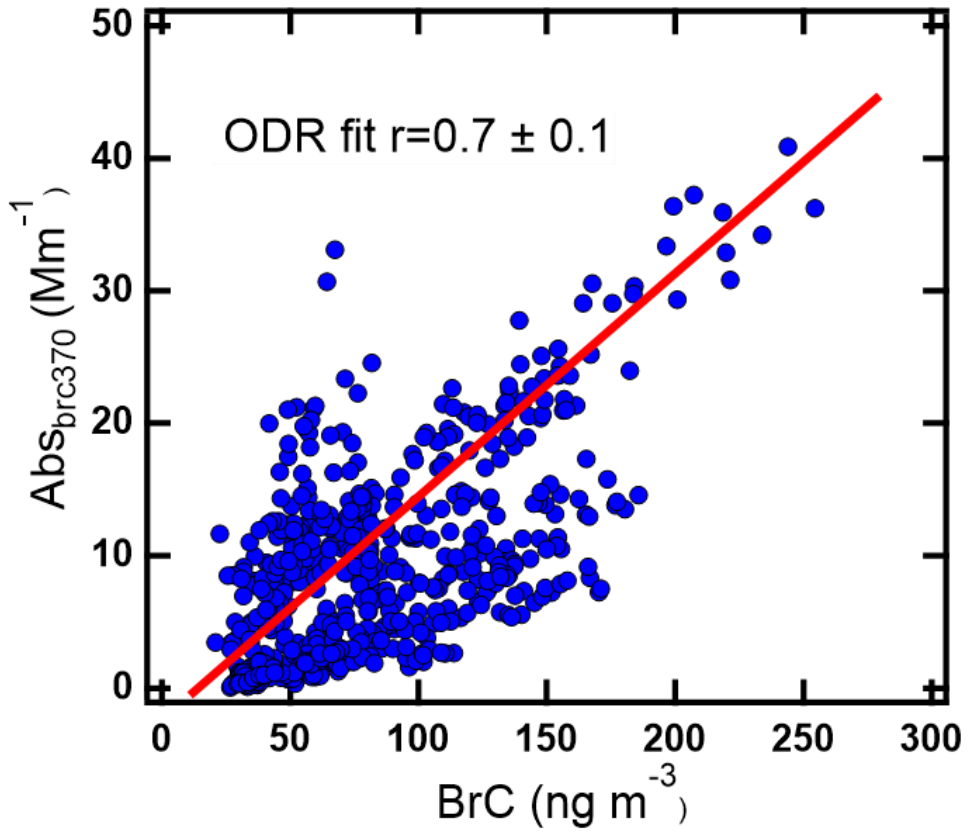

Figure S6. The correlation of 178 potential BrC mass (identified) and total BrC absorption (b_{brc370}).

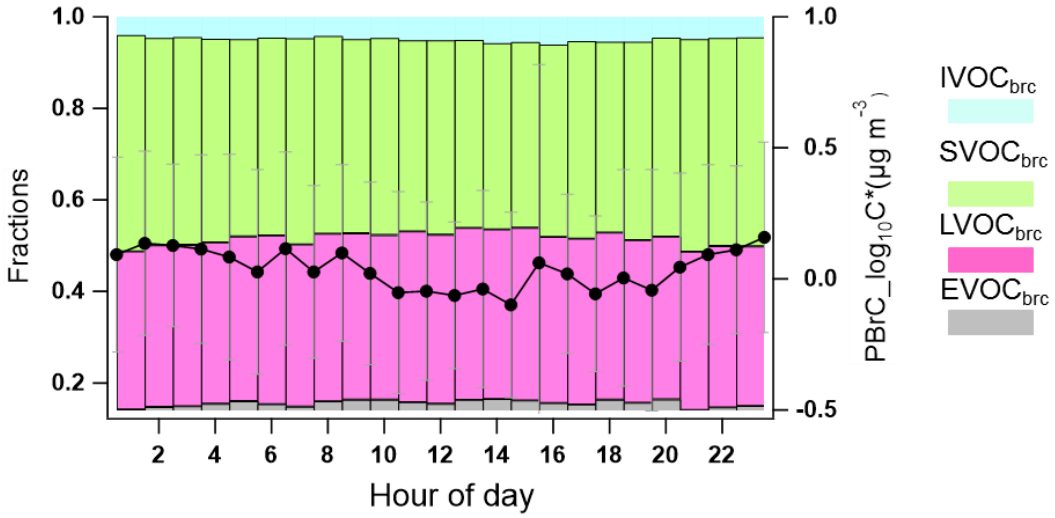

Figure S7. Diurnal profiles of $LVOC_{brc}$, $SVOC_{brc}$, $IVOC_{brc}$, $EVOC_{brc}$, and the average BrC volatility in the particle phase for the whole campaign (black circles).

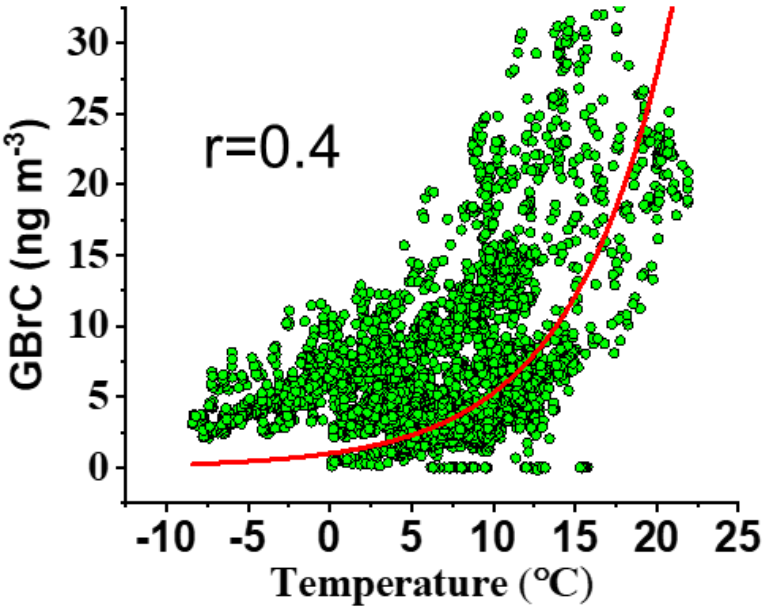

Figure S8. The correlation of gas-phase BrC and temperature based on exponential fit ($y=e^{(-0.17*x)}$)

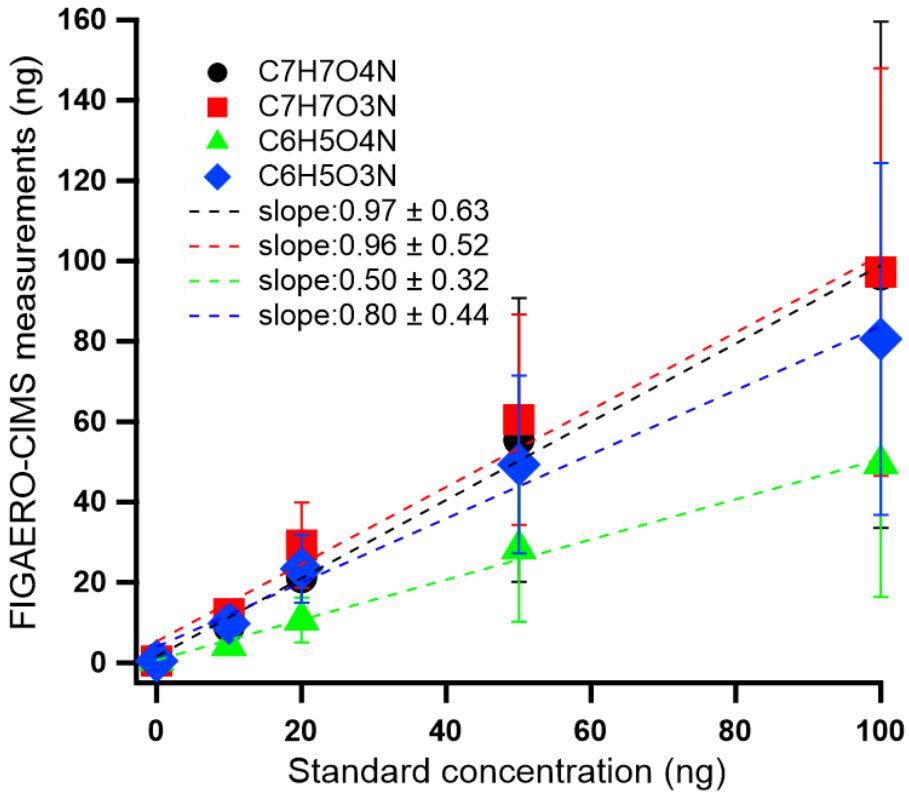

Figure S9. Calibration of FIGAERO-CIMS with four different nitro aromatic compounds. Blue: 4-nitropehnol; Green: 4-nitrocatechol; Red: 2-methyl-4-nitropehnol; Black: 4-methyl-5-nitrocatechol. The sensitivity of our iodide CIMS for 4-nitrophenol, 4-nitrocatechol, 2-methyl-4-nitropehnol, and 4-methyl-5-nitrocatechol were 18 ± 10 cps ppt^{-1}, 11 ± 7 cps ppt^{-1}, 21 ± 11 cps ppt^{-1}, and 21 ± 14 cps ppt^{-1}, respectively.

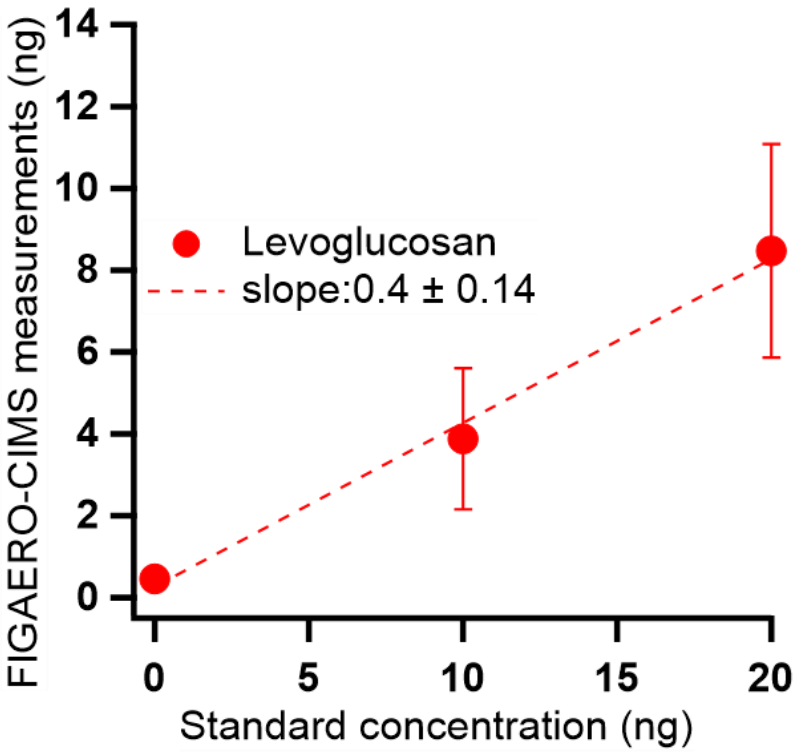

Figure S10. A calibration of FIGAERO-CIMS with levoglucosan. The measurement concentrations are calculated using a maximum sensitivity of 22 cps ppt^{-1} (Salvador et al., 2021). The sensitivity of levoglucosan was determined 9 ± 3 cps ppt^{-1}.

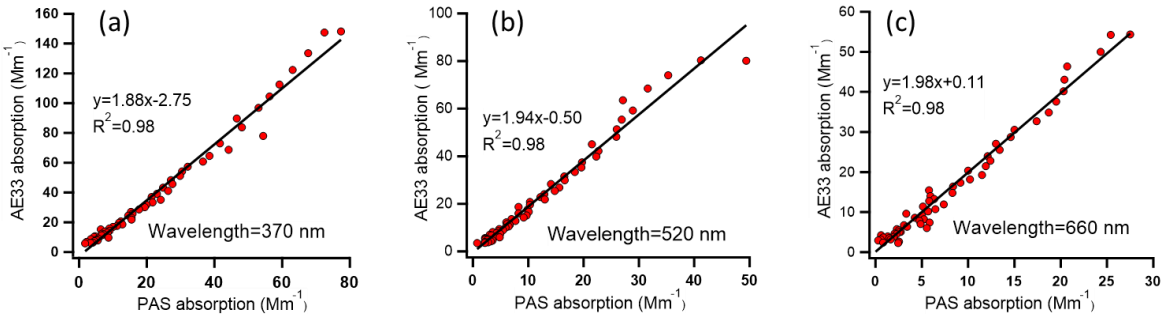

Fig. S11. Comparison of aerosol absorption coefficient measured by the photoacoustic spectrometer (PAS) and the aethalometer AE33 at 370 nm (a), (b), 520 nm, and 660 nm (c).

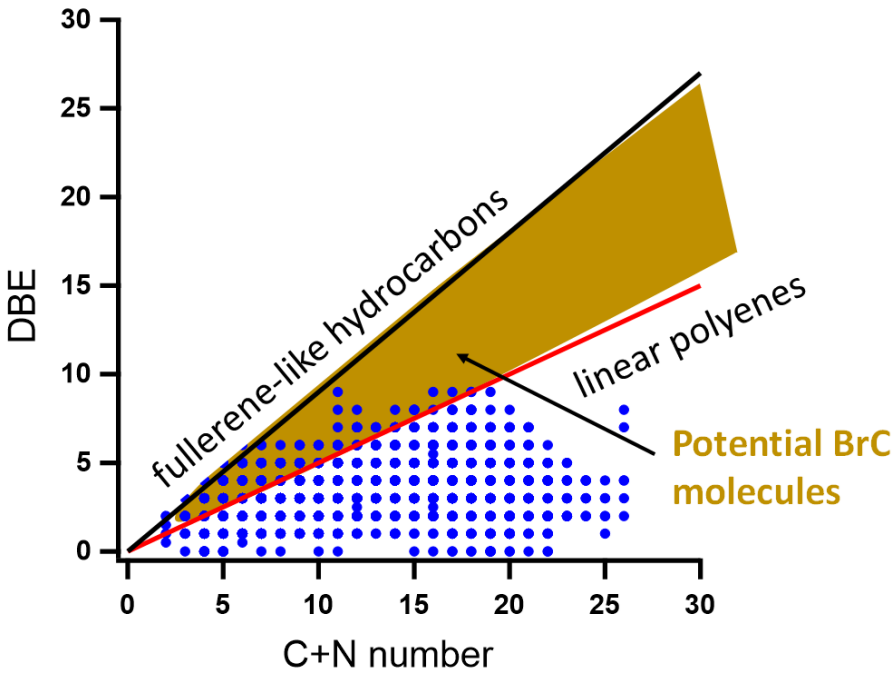

Figure S12. Plot of the double bond equivalent (DBE) vs numbers of carbon and nitrogen atoms according to our measurements following the procedure described by Lin et al., (2018). The lines indicate DBE reference values of linear conjugated polyenes (red solid line) and fullerene-like hydrocarbons with DBE=0.9*C (black solid line). Data points inside the yellow shaded area are potential BrC molecules. (cf. Lin et al., 2018).

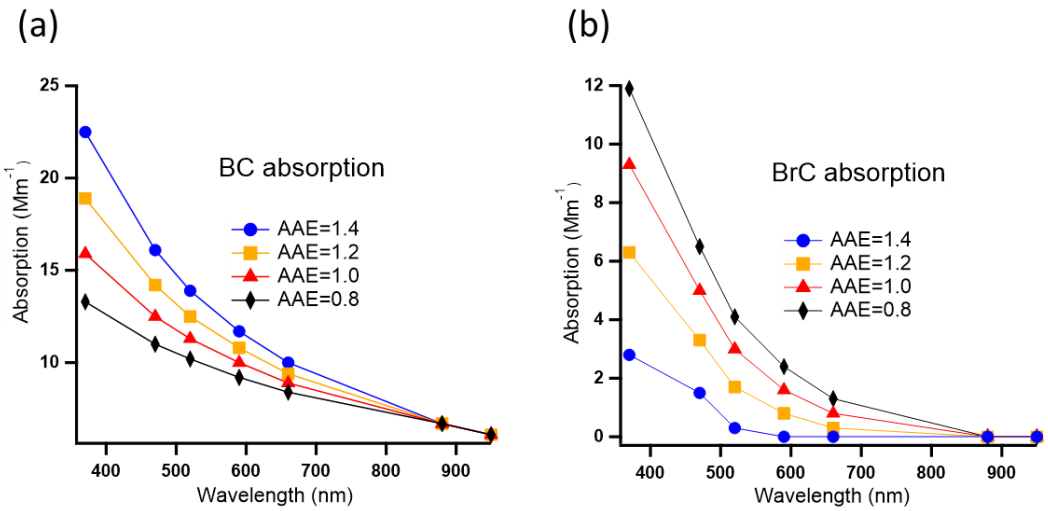

Figure S13. Light absorption of BC (a) and BrC (b) under different assumptions regarding the AAEBC. The blue, yellow, red, and black makers represent light absorption of BC and BrC when AAEBC is 1.4, 1.2, 1.0, and 0.8, respectively.

Reference

Cuevas-Agulló, E., Barriopedro, D., García, R. D., Alonso-Pérez, S., González-Alemán, J. J., Werner, E., Suárez, D., Bustos, J. J., García-Castrillo, G., García, O., Barreto, Á., and Basart, S.: Sharp increase in Saharan dust intrusions over the western Euro-Mediterranean in February–March 2020–2022 and associated atmospheric circulation, Atmos. Chem. Phys., 2023, 1-39, https://doi.org/10.5194/acp-24-4083-2024. 2024.

Lin, P., L. T. Fleming, S. A. Nizkorodov, J. Laskin, and A. Laskin.: Comprehensive Molecular Characterization of Atmospheric Brown Carbon by High Resolution Mass Spectrometry with Electrospray and Atmospheric Pressure Photoionization, Anal. Chem., 90, 12493-502, https://doi.org/10.1021/acs.analchem.8b02177, 2018.

Salvador, C. M. G., R. Z. Tang, M. Priestley, L. J. Li, E. Tsiligiannis, M. Le Breton, W. F. Zhu, L. M. Zeng, H. Wang, Y. Yu, M. Hu, S. Guo, and M. Hallquist.: Ambient nitro-aromatic compounds - biomass burning versus secondary formation in rural China, Atmos. Chem. Phys., 21, 1389-406, https://doi.org/10.5194/acp-21-1389-2021, 2021.

Xie, M., Chen, X., Hays, M. D., Lewandowski, M., Offenberg, J., Kleindienst, T. E., and Holder, A. L.: Light Absorption of Secondary Organic Aerosol: Composition and Contribution of Nitroaromatic Compounds, Environ. Sci. Technol., 51, 11607– 11616, https://doi.org/10.1021/acs.est.7b03263, 2017.